79-GT-130

an ASME publication

Determination of the Reynolds-Stress Tensor with a Single Slanted Hot-wire in Periodically Unsteady Turbomachinery Flow

P. KOOL

Research Assistant,
NFWO,
Vrije Universiteit Brussel,
Brussels, Belgium

The pitchwise distribution of the components of the Reynolds stress tensor downstream of a rotating blade row can be obtained with a single slanted hot-wire and the technique of periodic sampling and averaging. The requirements imposed on the hot-wire and the sensitivity coefficients to the six stresses are given. Information concerning the electronic set-up and the problems associated with measuring the Reynolds stresses are discussed. It is shown that the sampling technique does not modify the mean-square value of the sampled signal if the correlation time of the turbulence is smaller than half the sampling rate, or when the frequency bandwidth of the turbulence is higher than twice the sampling frequency. Typical results, including the 3D-mean flow data obtained downstream of a low-speed axial compressor rotor at different radii are presented. The results show typical modifications of the stresses in the rotor wake region and the regions influenced by secondary flow or tip-leakage flow.

Contributed by the Gas Turbine Division of The American Society of Mechanical Engineers for presentation at the Gas Turbine Conference & Exhibit & Solar Energy Conference, San Diego, Calif., March 12-15, 1979. Manuscript received at ASME Headquarters December 19, 1978.

Copies will be available until December 1, 1979.

THE AMERICAN SOCIETY OF MECHANICAL ENGINEERS, UNITED ENGINEERING CENTER, 345 EAST 47th STREET

Determination of the Reynolds-Stress Tensor with a Single Slanted Hot-wire in Periodically Unsteady Turbomachinery Flow

P. KOOL

NOMENCLATURE

A = parameter in the wire cooling law
A_u, A_v, A_w = sensitivity coefficient of the anemometer fluctuations to the turbulent velocity fluctuations u, v, w
B = parameter in the wire cooling law
d = differentiator symbol
E = anemometer voltage
e = fluctuations of the anemometer signal
f = frequency
H = transfer function of zero-order hold circuit
j = imaginary number
n = exponent in the wire cooling law, summation index
R = correlation function
S = blade pitch, power spectral function
s = coordinate in the blade-to-blade direction
t = time variable
T = period, energy
T^o = integration time
u = streamwise velocity fluctuation
v = normal velocity fluctuation, velocity component
$\bar{V}$ = average of steady velocity
w = binormal velocity fluctuation component
X, Y, Z = system of mutually perpendicular axis
= angle of flow vector
= Dirac delta function
^{2} = mean-square or variance of signal
= yaw angle of hot wire probe
= angular frequency
= time delay

= correlation
effective, relative to anemometer fluctuations
g = global
o = constant
p = probe
r = radial
s = sampled
t = turbulence
u = unsteadiness
x, y = along x, y coordinate axis
$\bar{}$ = overbar denotes average
= blade-to-blade average of time averaged signals
= absolute value
= turbulent component

INTRODUCTION

Recent turbomachinery research has been directed toward the effects of secondary flow, blade wake transport, end-wall and blade-boundary layers. The knowledge of the six components of the Reynolds shear stresses is essential for future detailed calculations of these viscous flow effects. As the end-wall and blade-boundary layers play an important role in the detailed flow calculations, the knowledge of the shear stresses in these layers and in the blade wakes is a key to the development of calculation methods. Especially since these layers are three-dimensional and since no general correlations are available for modeling these stresses, direct measurements are useful.

Turbulence measurements are even not restricted to the so-called viscous flow regions because, as was shown by Gorton and Lakshminarayana (1),[1] the classical assumption that the viscous and turbulence effects are confined to very thin regions near the blade surfaces is evidently inapplicable to inducers. The same is true for other types of machines when the end wall boundary

[1] Underlined numbers in parentheses designate References at end of paper.

layers are thick, when blade stalling occurs, or when large mixing regions are present due to secondary flow and/or tip-leakage flow.

An early contribution to the study of turbulence effects in turbomachinery was made by Kiock (2), which led to the definition of a disturbance and a turbulence level. His paper and the paper by Evans (3) only dealt with the streamwise velocity fluctuations, though the results can be easily extended to include the effects of the large changes in flow angles. The results of Raj and Lakshminarayana (4) confirm that none of the six stresses are usually neglectable, and the results of Eckardt (5) for a radial impeller show that turbulence measurements are a good indication of the onset and the presence of flow separations. Turbulence measurements downstream of the rotor of an axial compressor stage subjected to non-uniform inlet flow (6) stress the importance and the advantage of measuring the Reynolds stresses in interpreting and in following small details in the average flow data in the blade to blade flow. The close link between the turbulence signals and deviations from uniformity in the average flow make turbulence measurements an interesting tool in investigating the wake transport through successive blade rows (7).

Though the X-wire has been a favorite tool for turbulence measurements, a single hot-wire can be used to measure the six Reynolds stresses. The method was first introduced by Fujita and Kovasznay (8) for a straight wire, and it allowed to measure three stress components with a continuously rotating wire in a steady flow. Similar measurements of the six components with a slanted hot-wire were performed by Bissonnette and Mellor (9) in a steady flow. The method has been adapted by De Grande (10) to measurements in successive discrete positions. A similar method was used by Kool (11) for periodically unsteady flow in turbomachinery. The method is most easily explained in the case of a steady mean-flow vector, and it can easily be extended to oscillating flows by reducing the data with the technique of synchronous sampling (12). This sampling does not change the mean-square value of the signal if the correlation time of the sampled signal is smaller than half the sampling period (13). Therefore, no special devices are required to measure the mean-square and, hence, the turbulent stresses. The power spectrum of the input signal, on the other hand, is modified by the sampling process.

THE BASIC METHOD

It is well known that, except for particular orientations, a hot-wire is sensitive to the three components of the turbulent and/or unsteady velocity fluctuations of a flow. If these fluctuations are small, the equations describing the cooling of the hot-wire can be linearized to obtain a relation between the anemometer voltage fluctuation, e, and the three velocity fluctuations, u,v,w:

$$e = A_u \tilde{u} + A_v \tilde{v} + A_w \tilde{w} \qquad (1)$$

The sensitivity coefficients A_u, A_v, A_w depend on the wire orientation with respect to the mean flow vector and the wire cooling laws. We will derive these coefficients for a slanted hot-wire making use of the least sophisticated cooling laws to demonstrate the principle. Upon squaring and averaging equation (1), we obtain the mean-square value of the anemometer fluctuations.

$$\overline{e^2} = A_u^2\overline{\tilde{u}^2} + A_v^2\overline{\tilde{v}^2} + A_w^2\overline{\tilde{w}^2} + 2A_uA_v\overline{\tilde{u}\tilde{v}} + 2A_uA_w\overline{\tilde{u}\tilde{w}} + 2A_vA_w\overline{\tilde{v}\tilde{w}} \qquad (2)$$

The mean-square contains information on all stresses. If the orientation of the wire is modified, an equation similar to equation (2) is obtained with different values for the sensitivity coefficients. If six different orientations are realized, the turbulent stresses can be calculated from the six linear equations with the six mean-square values as data. It is better to use more than six data and to solve the system of equations by least squares fitting. Linear algorithms can be used, but general optimization procedures are useful if the system of equations is nonlinear. It is evident that the use of a single hot-wire puts a constraint on the possible combination of values for the sensitivity coefficients in equation (2). The sensitivity to the mixed stresses can be increased if two wires are used. The first one can be oriented to obtain a maximum value for, say, A_u, the other one for A_v. If the anemometer fluctuations are multiplied and averaged a high sensitivity to the $\overline{uv}$ stress is obtained.

The method proposed to Fujita (8) makes use of a continuous record of the mean-square signal. The present method uses discrete positions and discrete values of the mean-square. It is an improvement of the previous method because the wire is stationary with respect to the flow while the meter is averaging. Moreover, the rotation of the wire itself can induce a mean-square signal,

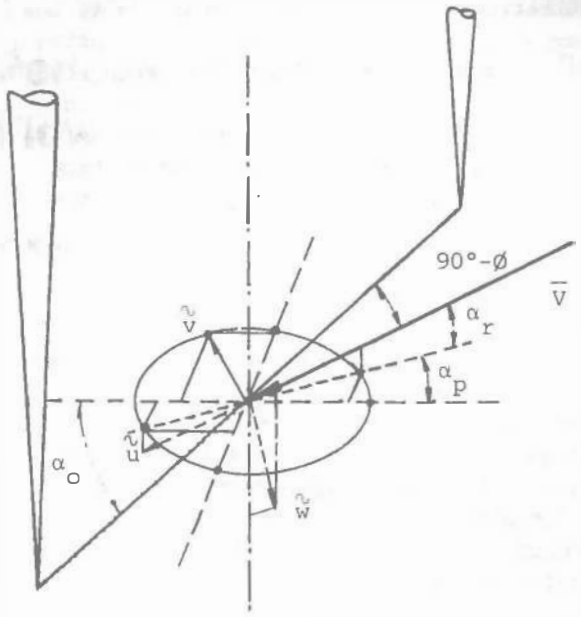

Fig. 1 Hot-wire configuration with average velocity $\bar{V}$ and turbulent components u,v,w in the streamwise, normal, and binormal direction. The angle, α_p, between the plane, of the wire and the prongs, and the projection of the velocity vector is shown negative

and the rotating wire system cannot be used together with the technique of periodic sampling and averaging in periodically unsteady flows.

SLANTED WIRE SENSITIVITY

In the following, we derive the sensitivity coefficients of a slanted hot-wire in a steady flow with mean velocity $\bar{V}$ and turbulent fluctuations u,v,w as depicted in Fig. 1 assuming simple cooling laws for the demonstration.

In a limited velocity range, the cooling of a hot-wire by an effective velocity is satisfactorily described with King's law

$$E^2 = A + Bv_e^n \tag{3}$$

The effective velocity is related to the velocity modulus and the yaw-angle, , by the cosine law

$$v_e = |v|\cos(\phi) \tag{4}$$

The yaw angle, , is written as function of the probe turning angle, α_p, the radial angle, α_r, and the slant angle, α_o

$$\sin\phi = \cos\alpha_o \cos\alpha_r \cos\alpha_p + \sin\alpha_o \sin\alpha_r \tag{5}$$

If the u,v,w -fluctuations are small, we can write

$$d\alpha_p = \frac{\tilde{v}}{|v|} \tag{6}$$

$$d\alpha_r = \frac{\tilde{w}}{|v|} \tag{7}$$

$$d|v| = \tilde{u} \tag{8}$$

$$|v| = \bar{v} \tag{9}$$

According to equation (1), we have

$$e = \frac{\partial E}{\partial \alpha_p} d\alpha_p + \frac{\partial E}{\partial \alpha_r} d\alpha_r + \frac{\partial E}{\partial |v|} d|v| \tag{10}$$

Through equations (4), (5) and (9), it is easy to obtain the sensitivity coefficients

$$A_u = \frac{n(E^2 - A)}{2E\bar{V}} \tag{11}$$

$$A_v = A_u \frac{tg\phi \cos\alpha_o \cos\alpha_r \sin\alpha_p}{\cos\phi} \tag{12}$$

$$A_w = A_u \frac{\cos\alpha_o \sin\alpha_r \cos\alpha_p - \sin\alpha_o \cos\alpha_r}{\cos\phi} tg\phi \tag{13}$$

The most obvious way to modify the orientation of the wire with respect to the velocity vector is by rotating the hot-wire probe around its axis into different positions which corresponds to a variation of the angle, α_p. The other parameters are not modified by this change. This rotation is most easily performed by using a stepping motor which allows discrete positions with respect to a fixed reference frame.

Typical sensitivity coefficients and their products are shown in Fig. 2 as function of the probe angle. The sensitivity, A_u and A_v, behave similarly, but the wire is more sensitive to streamwise fluctuations. The parameter, A_w, reaches a maximum value when the probe angle is zero. In this position, the velocity vector lies in the plane of the hot-wire and the prongs. As can be seen in Fig. 3, the hot-wire calibration curve is strongly nonlinear in this region when the angle, α_o, is small and the region should be avoided. The sensitivity to the stresses, uv and vw, is very similar and the sensitivity to the uw component is larger. The similarity of the uv and vw coefficients in equation (2) makes both

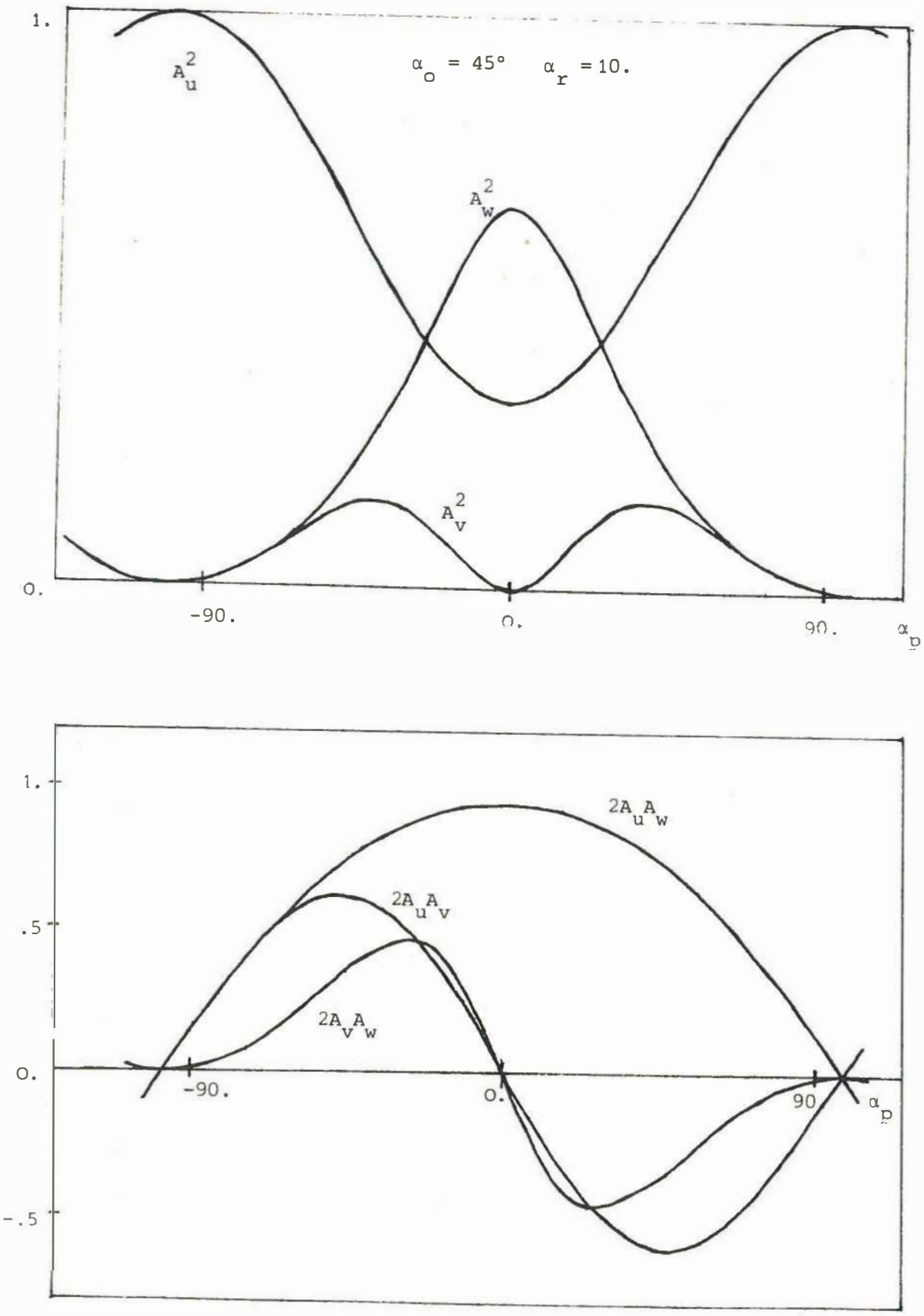

Fig. 2 Sensitivity coefficients of a 45-deg slanted hot-wire to the six Reynolds stresses for a velocity inclined at an angle of 10 deg for various values of the probe turning angle

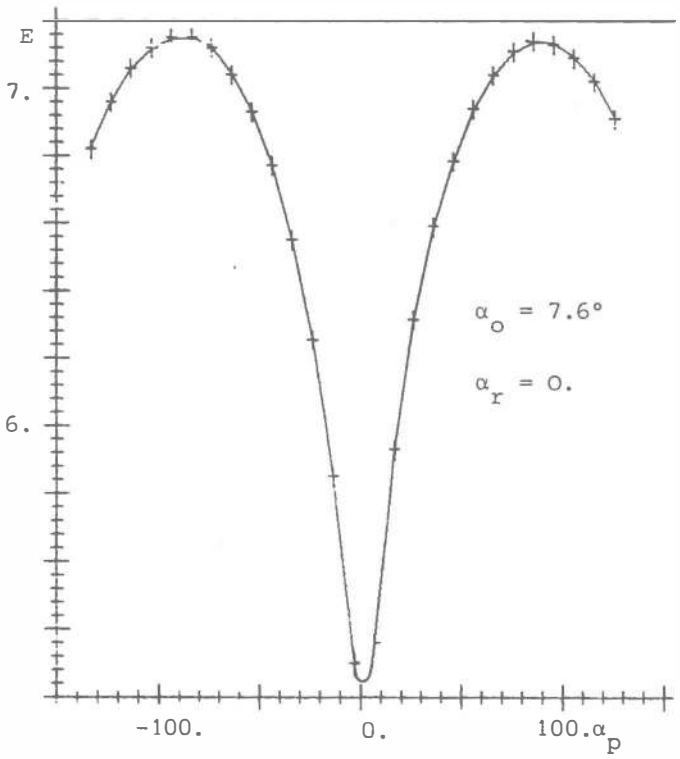

Fig. 3 Angular calibration curve of a hot-wire with small slant angle to show the nonlinearity close to zero probe angle

stresses more difficult to discern if insufficient data are taken in the region where both curves differ. The A_v and A_w coefficients are zero at an angle, $_p$, which differs from 90 deg because the radial angle, $_r$, is not zero. The slanted wire is most sensitive to the v^2 component of the Reynolds stress at an angle, $_p$, approximately equal to the slant angle, $_o$, of the wire. The sensitivity to the V^2-component can be increased by using a lower slant angle.

APPLICATION TO PERIODIC FLOW

Experimental Setup

Fig. 4 shows the basic setup of the instruments. The hot-wire anemometer signal downstream of a rotating blade row varies periodically in time due to the nonuniform blade-to-blade flow at rotor exit but also contains random turbulent fluctuations. By sampling this signal with a sample-and-hold circuit at the blade passing frequency, we can extract the periodic blade-to-blade information, $\bar{E}(s)$, where s represents the blade-to-blade coordinate (12). The three-dimensional mean-flow data are computed from this average anemometer signal. To calculate the blade-to-blade evolution of the Reynolds

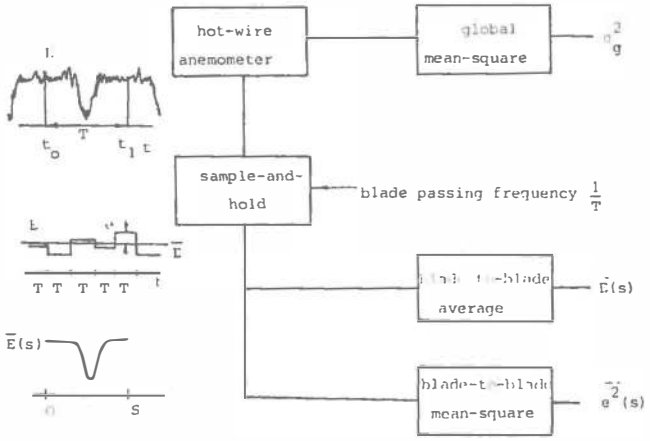

Fig. 4 Setup of the instruments to measure the blade-to-blade evolution of the periodic mean voltage and the periodic mean-square of the anemometer signal of a fixed probe downstream of a rotor

stresses, we must know the blade-to-blade evolution of the mean-square value of the anemometer fluctuations. In Fig. 4, the periodic signal is sampled at time t_o, t_1. The sample-and-hold circuit fixes his output level at the input level which is present at the sampling times t_o, t_1, and holds this level at the same value each time during T seconds following the sampling instant. The resulting stepwise changing signal is shown in Fig. 4. The time-average of this signal represents the average voltage level of the input signal, E, at the sampling moments t_o, t_1 ..... and it is denoted as $\bar{E}(o)$. To obtain the periodic component which is present in the anemometer signal, we must scan the whole period, T, by changing the time instant, t_o, where sampling is started. This is done by changing the phase of the sampling pulses with respect to the signal. In our system, the period, T, is subdivided into N regularly spaced points and the average voltage is determined in each of these points. The circuit switches from one point to the next one as soon as the average is determined and registrated. As such the periodic voltage, $\bar{E}(s)$, is obtained. During the integration process whereby the average is determined, we also measure the mean-square value of the fluctuations, e, around this average level. This mean-square signal also varies periodically in the blade-to-blade coordinate. A single blade-to-blade evolution of the mean-square and the average voltage is not sufficient to calculate the blade-to-blade velocity and Reynolds stress distribution. Therefore, we must repeat the foregoing process for a different orientation of the wire with re-

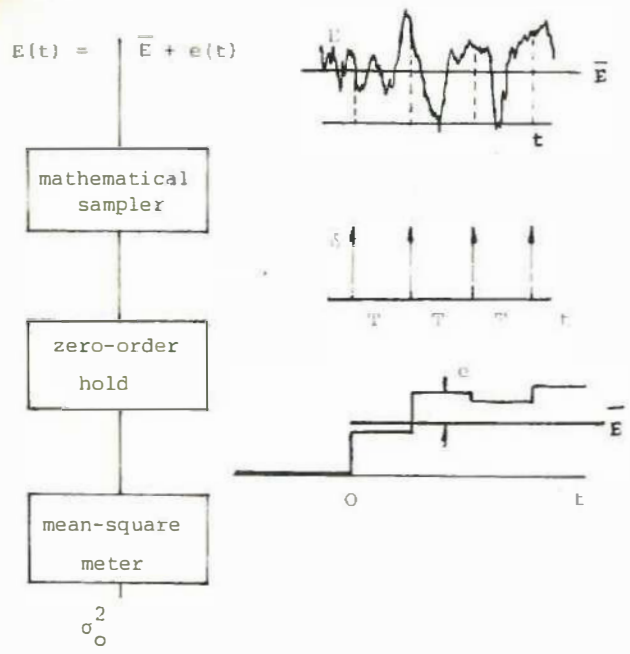

Fig. 5 Mathematical model used to describe the sampling action on a random input signal

spect to the flow at least six times. To show when the mean-square of the stepwise changing signal which is obtained at the output of the sample-and-hold circuit faithfully reproduces the mean-square value of the fluctuations of the input signal, we calculate the modifications of the power spectrum and the correlation function of a stationary random signal with non-zero mean applied to a sample-and-hold circuit.

THE SAMPLING PROCESS

Fig. 5 shows the mathematical model which is used to describe the action of the electronic circuit of Fig. 4, while it is averaging the signal in a given point in the blade-to-blade space. An aperiodic stationary random signal, E(t), of time is applied to a mathematical sampler which delivers a series of Dirac delta functions and the output is fed to a zero order-hold circuit. As in Fig. 4, the output levels are the fixed levels corresponding to the input signal level at the sampling instances, which are T seconds apart. The time-average of the input signal is $\bar{E}$, and it is also the time-average of the stepwise changing output signal. Therefore, the average signal level changes from zero to $\bar{E}$ when the sampling is started. The mean-square meter responds to this transient. Depending upon the time constant of the meter which is fixed by setting the integration time, this transient indication will die out. It is an unavoidable and unwanted phenomena while we are interested in the mean-square intensity of the fluctuations, e, around this average level, $\bar{E}$. The mean-square value is defined as

$$\sigma^2 = \lim_{T^o \to \infty} \frac{1}{T^o} \int_0^{T^o} e^2(t)dt = \overline{e^2} \qquad (14)$$

With the definition of the correlation function, R, as

$$R(\tau) = \lim_{T^o \to \infty} \frac{1}{2T^o} \int_{-T^o}^{+T^o} e(t)e(t-\tau)dt \qquad (15)$$

we immediately have

$$\sigma^2 = R(o) \qquad (16)$$

The Wiener-Khintchine Fourier transform relation between the correlation function and the power spectrum yields

$$S(\omega) = \int_{-\infty}^{+\infty} R(\tau)\exp(-j\omega\tau)d\tau \qquad (17)$$

with

$$\omega = 2\pi f = \frac{2\pi}{T} \qquad (18)$$

and

$$R(\tau) = \int_{-\infty}^{+\infty} S(f)\exp(j\omega\tau)df \qquad (19)$$

which yields an equivalent formula for the mean-square value

$$\sigma^2 = R(o) = \int_{-\infty}^{+\infty} S(f)df \qquad (20)$$

The sampling theorem (14) tells us that the output of the mathematical sampler is a signal with a series of Diract delta functions as correlation function

$$R_s(\tau) = \frac{1}{T} \sum_{n=-\infty}^{\infty} R(nT)\delta(\tau - nT) \qquad (21)$$

when the input signal is a stationary random function with correlation function, R, and with a sampling period, T.

The correlation time of the input signal is

a measure of the mean time during which the input signal fluctuations are correlated. Two fluctuations which are separated by a larger time difference can be considered as uncorrelated and the correlation function is practically zero for this time lag. The correlation time is usually defined as

$$T_c = \int_0^\infty \frac{R(\tau)}{R(o)}\, d\tau \tag{22}$$

If the correlation time is smaller than about half the sampling period

$$T_c < \frac{T}{2} \tag{23}$$

then equation (21) reduces to

$$R_s(\tau) = \frac{R(o)}{T}\,\delta(\tau) \tag{24}$$

or with equation (16)

$$R_s(\tau) = \frac{\sigma^2}{T}\,\delta(\tau) \tag{25}$$

The power spectrum corresponding to this correlation function is flat and given by equation (17)

$$S_s(\omega) = \frac{\sigma^2}{T} \tag{26}$$

The zero-order-hold circuit has a step response given by

$$H(\omega) \doteq \frac{1 - \exp(-j\omega T)}{j\omega} \tag{27}$$

The power spectrum at the output of the sample-and-hold is then given by

$$S_o(\omega) = S_s(\omega)\,|H(j\omega)|^2 \tag{28}$$

or

$$S_o(\omega) = \sigma^2 T\,\frac{\sin^2(\frac{\omega T}{2})}{(\frac{\omega T}{2})^2} \tag{29}$$

Most of the energy is now concentrated in the frequency band

$$o \leq f \leq \frac{1}{2T} \tag{30}$$

The zero-order-hold circuit acts as a low-pass filter and the sampling process indeed stretches the signal in time and the longer the sampling period, T, the more the signal behaves like a low frequency signal. Therefore, the mean-square meter must have a flat frequency response up to very low frequencies because the signal energy is concentrated at and around zero frequency by the sampling action. The mean squar of the output signal according to equation (20) is then

$$\sigma_o^2 = \sigma^2 T \int_{-\infty}^{\infty} \frac{\sin^2(\frac{\omega T}{2})}{(\frac{\omega T}{2})^2}\, df \tag{31}$$

The integral is given in mathematical tables and the expression reduces to

$$\sigma_o^2 = \sigma^2 \tag{32}$$

which shows that the mean-square value is not modified if the criterium (23) is fulfilled. A short correlation time is equivalent to the requirement of a high bandwidth. In turbomachinery, the turbulence spectrum can be expected (3) to reach far beyond twice the blade passing frequency, 2/T, which corresponds to the right-hand side of equation (23). Equation (29) shows that the power spectrum is always modified by the sampler but the total energy is the same.

BLADE-TO-BLADE SIGNAL RECOVERY

Another requirement which must be satisfied is the Shannon criterium which tells us that if we want to obtain the evolution of the blade-to-blade signal, then we must have at least two points within a period of the highest frequency signal which is present in the signal waveform. If the blade-to-blade velocity signal were a sinusoidal function of the blade-to-blade coordinate, two data points would suffice to describe this sine function. In practice, one will, of course, take a lot more points because one does not know the velocity to be sinusoidal in advance. One should realize that the blade-to-blade evolution of the turbulent stresses usually represents a signal with a higher frequency limit than the velocity signal. The profiles of Reference (4) and our results are a typical example. Therefore, the stress evolution must be reconstructed in up to two or four times as much points within a blade pitch as the velocity signal is.

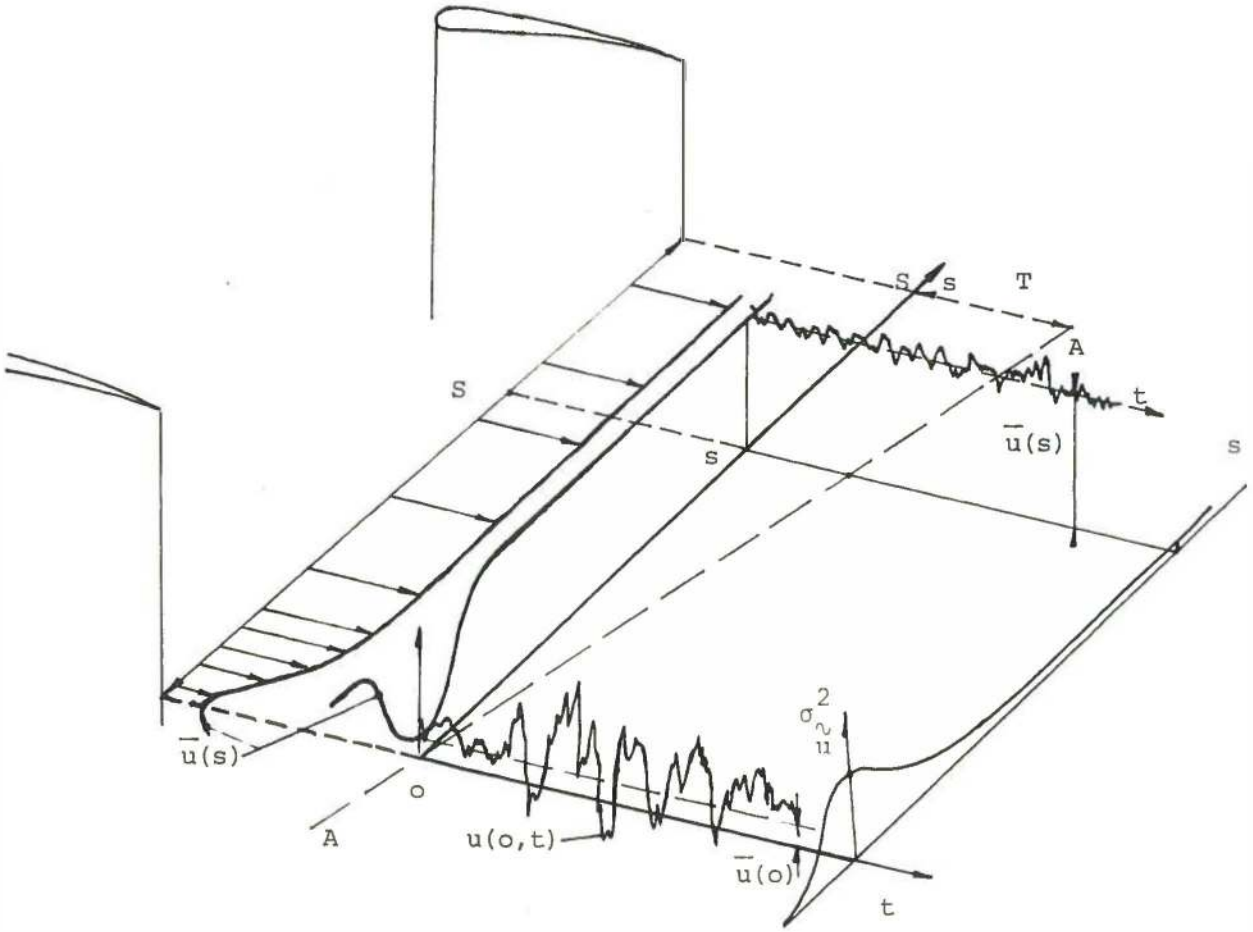

Fig. 6 Distribution in the blade-to-blade and time coordinate of the instantaneous velocity fluctuating around its time averaged mean value and the blade-to-blade distribution of the intensity of these fluctuations and the average flow

VERIFICATION OF RESULTS

Two tests can be performed to verify the measured blade-to-blade mean-square distribution of the anemometer signal and to check the validity of the obtained Reynolds stresses. The latter must indeed satisfy the inequality

$$-1 \leq \frac{\overline{\tilde{u}\tilde{v}}}{\sqrt{\overline{\tilde{u}^2}}\sqrt{\overline{\tilde{v}^2}}} \leq 1 \qquad (33)$$

Two other relations are derived by permutation of the variables, u,v,w.

Another useful relation is derived from Kiock's relation (2)

$$T_g^2 = T_u^2 + T_t^2 \qquad (34)$$

This equation states that the sum of the energies of the turbulent velocity fluctuations and the variations in mean velocity is equal to the energy of the overall velocity fluctuations. The velocity is, therefore, split up in a periodic blade-to-blade component and a turbulent component which varies in time in each point of the blade-to-blade space (s-coordinate)

$$u(s,t) = \bar{u}(s) + \tilde{u}(s,t) \qquad (35)$$

To have a better picture of the different flow variables, Fig. 6 shows a stationary blade row and the nonuniform exit flow.

In each point fixed by the blade-to-blade coordinate, s, the instantaneous velocity oscillates in time around its average level, $\bar{u}$, and this is shown for two different points, one within the blade wake and one out of the wake region. Within the wake the turbulent fluctuations are higher; therefore, the signal fluctuates violently around the average level, $\bar{u}(o)$. We can measure the mean-square according to equation (14) with a mean-square meter with integra-

tion time T^o

$$\sigma^2_{\tilde{u}}(s) = \frac{1}{T^o}\int_o^{T^o} \tilde{u}^2(s,t)dt \qquad (36)$$

and obtain the periodic blade to blade evolution of the mean-square signal as shown in Fig. 6.

If the cascade were rotating, then we would have to use a rotating wire to measure the signal, u(s,t), as a function of time. A hot-wire fixed in a stationary frame of reference cannot give us this signal completely. The hot-wire signal is indeed obtained by cutting the u(s,t) space along the line, AA. The period, T, corresponds to the time necessary for one blade passage to come across the wire. The signal, u(o,t), is seen by the hot wire at time zero for the first time and it will be seen by the wire after a complete revolution of the rotor. If it is N-bladed, the time elapse is given by

$$T_o = NT \qquad (37)$$

If we want the particular channel depicted in Fig. 6 to be investigated by periodic sampling and averaging, we will sample the hot-wire signal at time zero and every T_o seconds afterward. The mean-square of the fluctuations will be measured correctly according to equation (23) if the correlation time of the signal, u(o,t), satisfies the inequality

$$T_c < \frac{T_o}{2} \qquad (38)$$

In practice, we must, therefore, take the maximum possible correlation time of all signals u(s,t) within the blade pitch as the sampling is scanned through the blade-to-blade space, and test the inequality (38). If all blade passages are averaged, the sampling rate increases and the condition is more severe but should not give problems in turbomachinery.

We can now write the contribution of the turbulent energy to relation (34) as

$$T_t^2 = \frac{1}{S}\int_o^S \sigma^2_{\tilde{u}}(s)ds \qquad (39)$$

whereas the contribution of the fluctuations in mean velocity around the average mean is given by

$$T_u^2 = \frac{1}{S}\int^S (\bar{u}^2(s) - \bar{\bar{u}}^2)ds \qquad (40)$$

with

$$\bar{\bar{u}} = \frac{1}{S}\int_o^S \bar{u}(s)ds \qquad (41)$$

We can write down equations (34) through (41) for the anemometer voltage, E, which is written as the sum of a periodic mean voltage and a turbulent component

$$E(s,t) = \bar{E}(s) + e(s,t) \qquad (42)$$

The energy of the overall fluctuations is measured as in Fig. 4 with a mean-square meter connected to the anemometer. The contribution of the periodic component is integrated according to equations (40) and (41), whereas the contribution of the random fluctuations is obtained by pitch averaging the measured mean-square value over the blade-pitch

$$T_e^2 = \frac{1}{S}\int_o^S \overline{e^2}(s)ds \qquad (43)$$

Our results confirm the relation (34) of Kiock to within 3 percent and it was used to check the validity of the data before reducing them to the final results.

EXTENSION OF THE KIOCK RELATION TO MIXED STRESSES

The original equation of Kiock (2) and the equation of Evans (3) do not include the effects of changes in the absolute flow angle as was pointed out by Evans, but neither contains the influence of the radial flow angle variation. These variations are taken into account in the extension of the Kiock relation when applied to the mixed stresses. One, therefore, decomposes the velocity vector into three components along three mutually perpendicular axis. If one of these components is written as

$$u_x(s,t) = \bar{u}_x(s) + \tilde{u}_x(s,t) \qquad (44)$$

where u_x represents the turbulent component which satisfies

components.

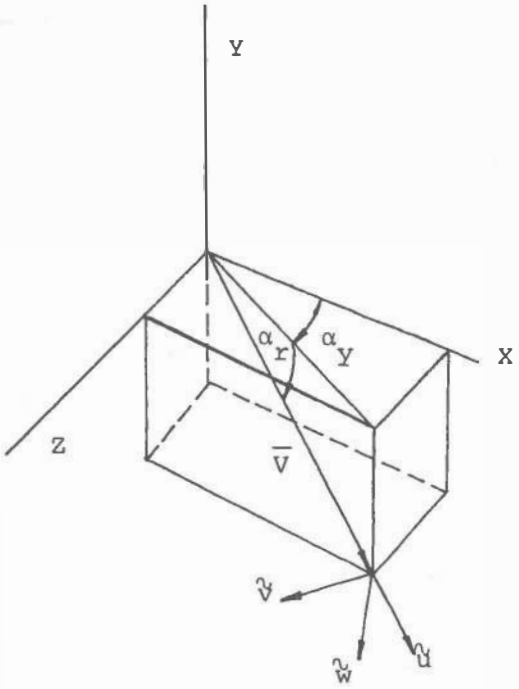

Fig. 7 Transformation of the turbulent velocity fluctuations to a new coordinate system X, Y, Z

$$\int_0^{T^\circ} \tilde{u}_x(s,t)\frac{dt}{T^\circ} = 0 \qquad (45)$$

and with $\bar{u}_x$ the periodic mean flow component.

Similarly

$$v_y(s,t) = \tilde{v}_y(s,t) + \bar{v}_y(s) \qquad (46)$$

Defining a global mean shear stress as

$$\overline{\overline{uv}} = \int_0^S\int_0^{T^\circ} u(s,t)v(s,t)\frac{dsdt}{S\ T^\circ} \qquad (47)$$

$$= \int_0^S\int_0^{T^\circ} \tilde{u}_x(s,t)\tilde{v}_y(s,t)\frac{dsdt}{S\ T^\circ} + \int_0^S \bar{u}_x(s)\bar{v}_y(s)\frac{ds}{S} + \int_0^S \bar{u}_x(s)\int_0^{T^\circ}\tilde{v}_y(s,t)\frac{dt}{T^\circ}\frac{ds}{S}$$

$$+ \int_0^S \bar{v}_y\int_0^{T^\circ}\tilde{u}_x(s,t)\frac{dt}{T^\circ}\frac{ds}{S} \qquad (48)$$

with equivalence (45), this expression reduces to

$$\overline{\overline{uv}} = \overline{\bar{u}_x\bar{v}_y} + \overline{\overline{\tilde{u}_x\tilde{v}_y}} \qquad (49)$$

The global stress can thus be considered as made up of a stress due to the unsteady velocity component and a stress due to the turbulent velocity

COORDINATE TRANSFORMATION

The (u,v,w) vector can be transformed to the X, Y, Z coordinate system depicted in Fig. 7 by the following matrix

$$\begin{vmatrix} \cos\alpha_r\cos\alpha_y & -\sin\alpha_y & -\sin\alpha_r\cos\alpha_y \\ -\sin\alpha_r & 0. & -\cos\alpha_r \\ \cos\alpha_r\sin\alpha_y & \cos\alpha_y & -\sin\alpha_r\sin\alpha_y \end{vmatrix} \qquad (50)$$

Squaring and averaging leads to a linear relation between the new stress and the six previous stresses, such as

$$\overline{\tilde{v}_y^2} = \overline{\tilde{u}^2}\sin^2(\alpha_r) + \overline{\tilde{w}^2}\cos^2(\alpha_r) + \overline{\tilde{u}\tilde{w}}\ 2\sin\alpha_r\cos\alpha_r \qquad (51)$$

As the scatter on the original stress terms is usually high, the newly calculated values present still higher scatter and systematic trends can be obscured quickly.

EXPERIMENTAL RESULTS

The results have been obtained in the R1 low-speed compressor of the Von Karman Institute as described in Reference (12). Present results correspond to a flow coefficient based on rotor tip speed of 0.45 and a pressure coefficient based on mean rotot speed of 0.68 and were obtained in an axial plane 0.47 chords downstream of the rotor outlet plane. The pitchwise evolution of the mean three-dimensional flow is determined with the method described in Reference (12) and the Reynolds stresses are obtained from six to eight different angular positions of the wire at each radial location.

The blade-to-blade evolution of the Reynolds stresses at three radii (20.8, 64.7, 74.9 percent blade height) are plotted in Figs. 8 to 13 and they have been scaled with the square of the absolute velocity. The radial flow angle is measured positive toward rotor-hub and is defined in Fig. 1 and plotted in Fig. 14. This is not the flow angle in a meridional plane. The blade-to-blade flow is further characterized by the absolute flow angle, Fig. 15, and the absolute velocity, Fig. 16. The profiles at 20.8 percent blade height are normal, but the velocity profile at 64.7 percent height is deformed at the suction

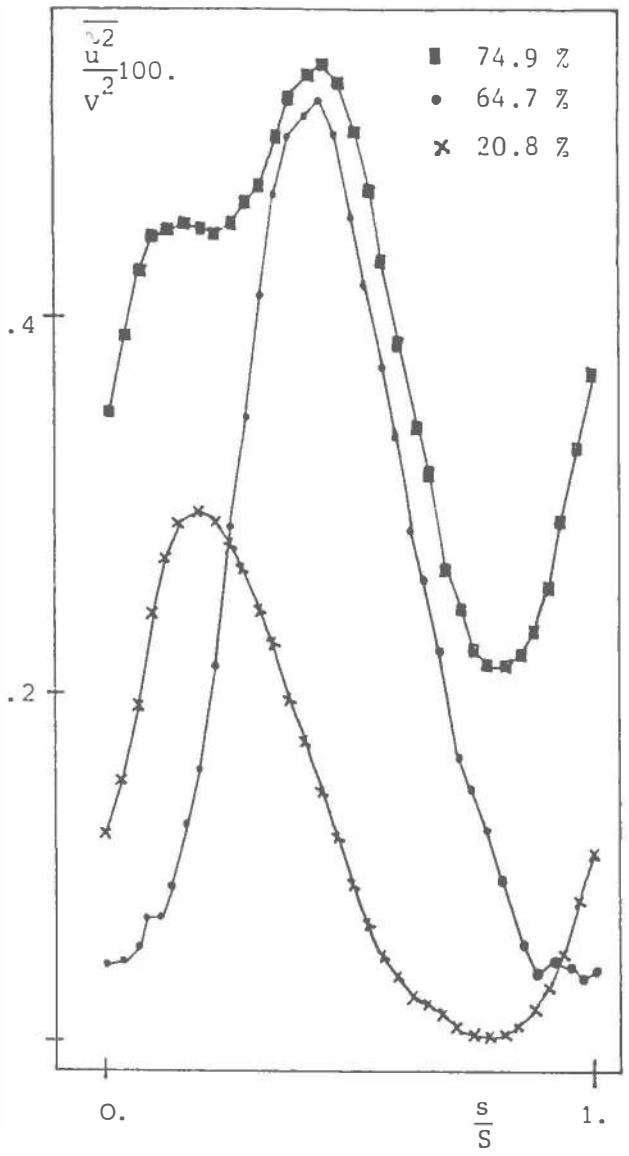

Fig. 8 Blade-to-blade evolution of the nondimensional streamwise turbulent intensity u^2 at three blade heights (20.8, 64.7, and 74.9 percent)

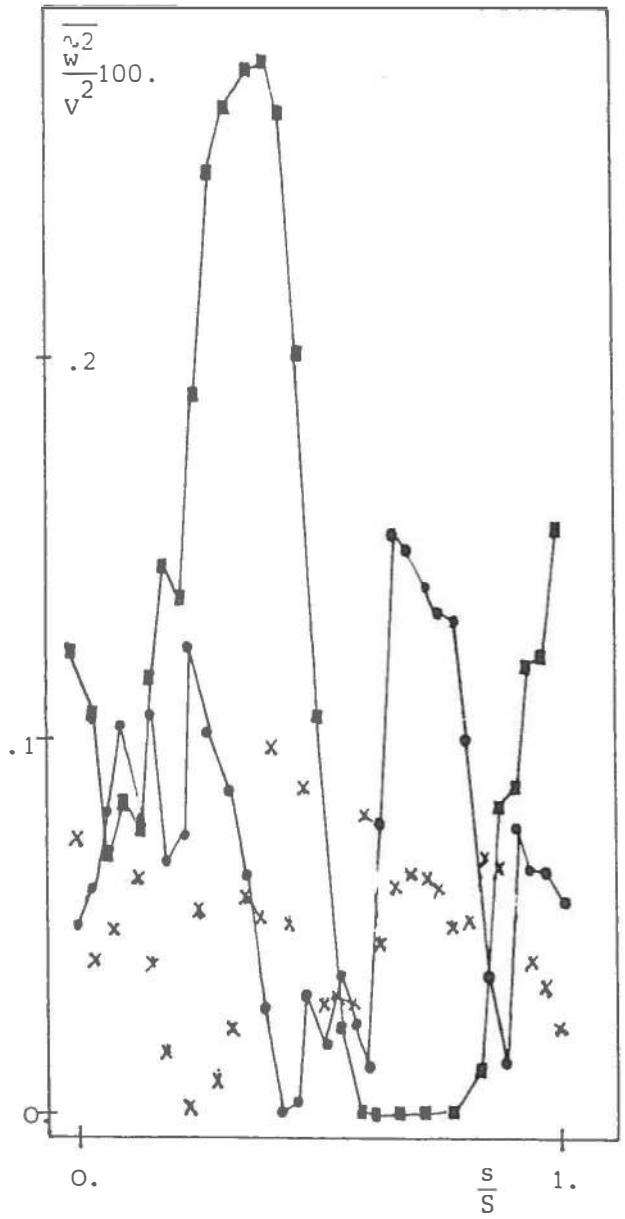

Fig. 9 Blade-to-blade distribution of the nondimensional turbulent intensity, w^2

side, and there is a disturbance at the pressure side of the wake at 74.9 percent height. The wake centerline shifts within a blade pitch due to the variation of mean flow angle in the radial direction. The v^2-stress is the largest one, and the w^2 component is normal to the end-walls and is the smallest one. The streamwise fluctuation intensity is high within the blade wake and the intensity increases with blade height. The disturbance at 64.7 percent height does not yield very high streamwise fluctuations. At 74.9 percent height, on the contrary, there is a marked increase near the pressure side. The w^2-component follows the same increasing trend with blade height, but this component is small at the center of the blade wake. In both disturbance regions, there is an increase in w^2 intensity which shows the presence of important radial fluctuations. The v^2 component is large and this shows that the fluctuations of the absolute flow angle are the most intense. As can be inferred from Fig. 15, the pitchwise fluctuations in flow angle are large, too. The scatter on the data is large for the v^2 component and might be due to the low sensitivity of the wire for this turbulence component. The v^2 intensity is also high in the disturbance regions.

The blade-to-blade averages of the mixed

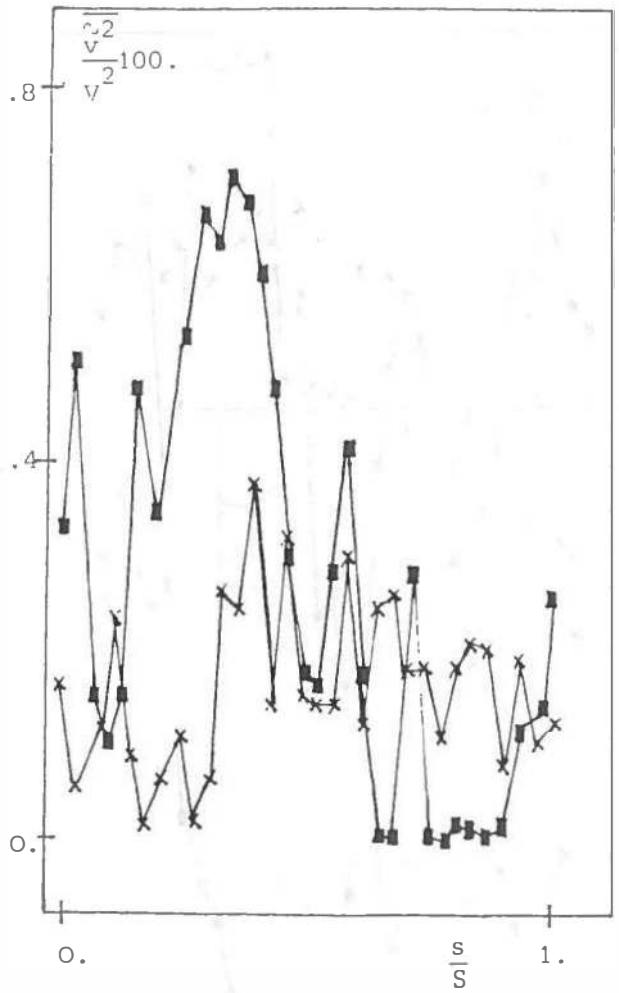

Fig. 10 Blade-to-blade distribution of the non-dimensional turbulent intensity, v^2

stresses are, in most cases, different from zero, and, therefore, there is a net contribution to the right-hand side of equation (49). The $\overline{vw}$ stress is positive most of the time and the $\overline{uv}$ stress profile has a nearly zero average except at 74.9 percent height where it becomes strongly negative. The increase of the $\overline{vw}$ stress at the pressure side at 74.9 percent height and at the suction side at 64.7 percent height is in agreement with the increased v^2 and w^2 values. At the blade centerline strong negative values of the $\overline{uw}$ stress are obtained. At 74.9 percent height, the $\overline{uw}$ stress is also negative in the disturbance region, whereas it is positive at 64.7 percent height. The $\overline{vw}$ stress is also high in the blade wake and in the disturbance region at the pressure side.

The blade wake is thus characterized by large streamwise fluctuations, and if we interpret the stresses as vorticity components, one can say that the vortices parallel to the end-

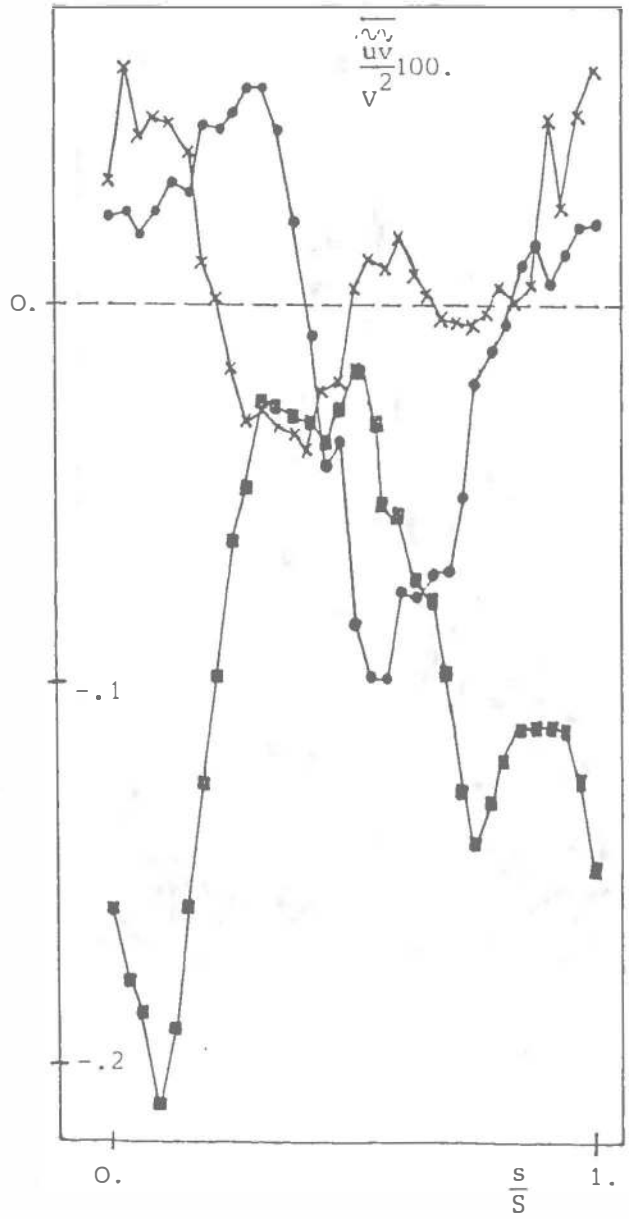

Fig. 11 Blade-to-blade distribution of the non-dimensional mixed stress, uv

wall are stronger than those normal to the wall. The velocity-defect regions, which are probably due to the presence of centrifugated blade boundary layer material accumulated by secondary flow effects, are characterized by increased fluctuations normal to the streamwise velocity and larger streamwise vorticity.

CONCLUSIONS

The Reynolds turbulent stresses and the apparent stresses due to the fluctuations in mean velocity can be measured with a single slanted hot-wire. The sensitivity coefficients of the

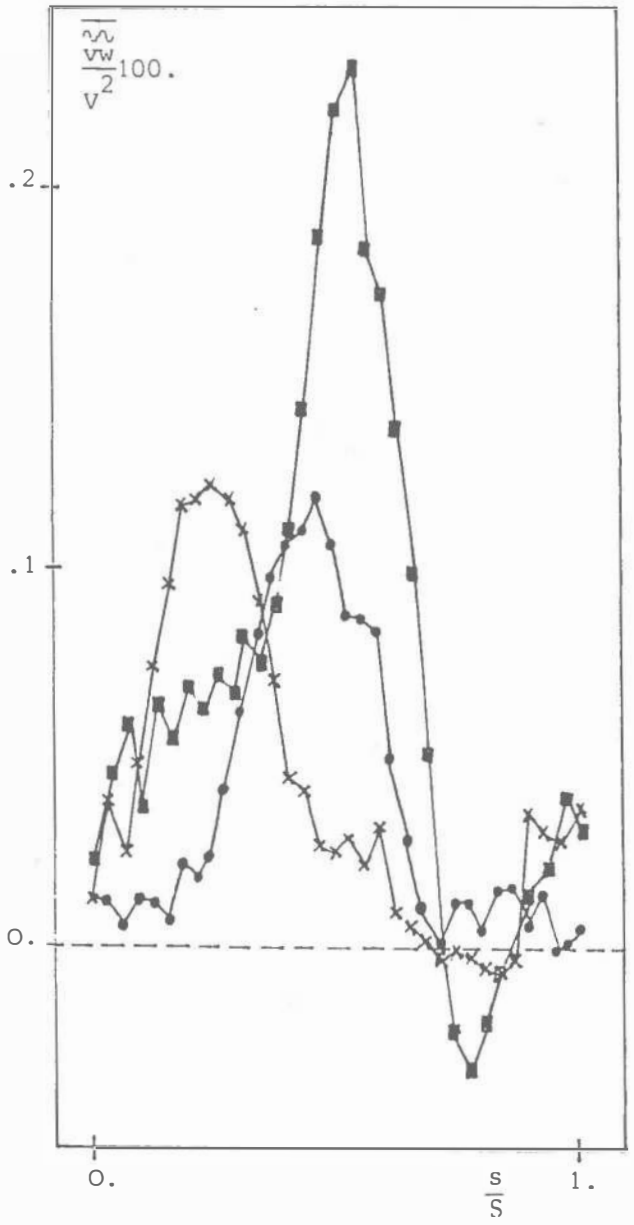

Fig. 12 Blade-to-blade distribution of the non-dimensional mixed stress, vw

anemometer fluctuations to the three turbulent velocity components are of interesting magnitude, and they can be varied by choosing different slant angles for the wire. The accuracy with which the six stresses are derived can be increased by providing more data than necessary and by solving the overdetermined system of equations with a least squares method.

For applications of the method to periodically unsteady flow, it is shown that the mean-square value of a turbulent signal can be obtained at the output of a sample-and-hold circuit if the turbulent signal has a power-bandwidth higher than twice the sampling frequency.

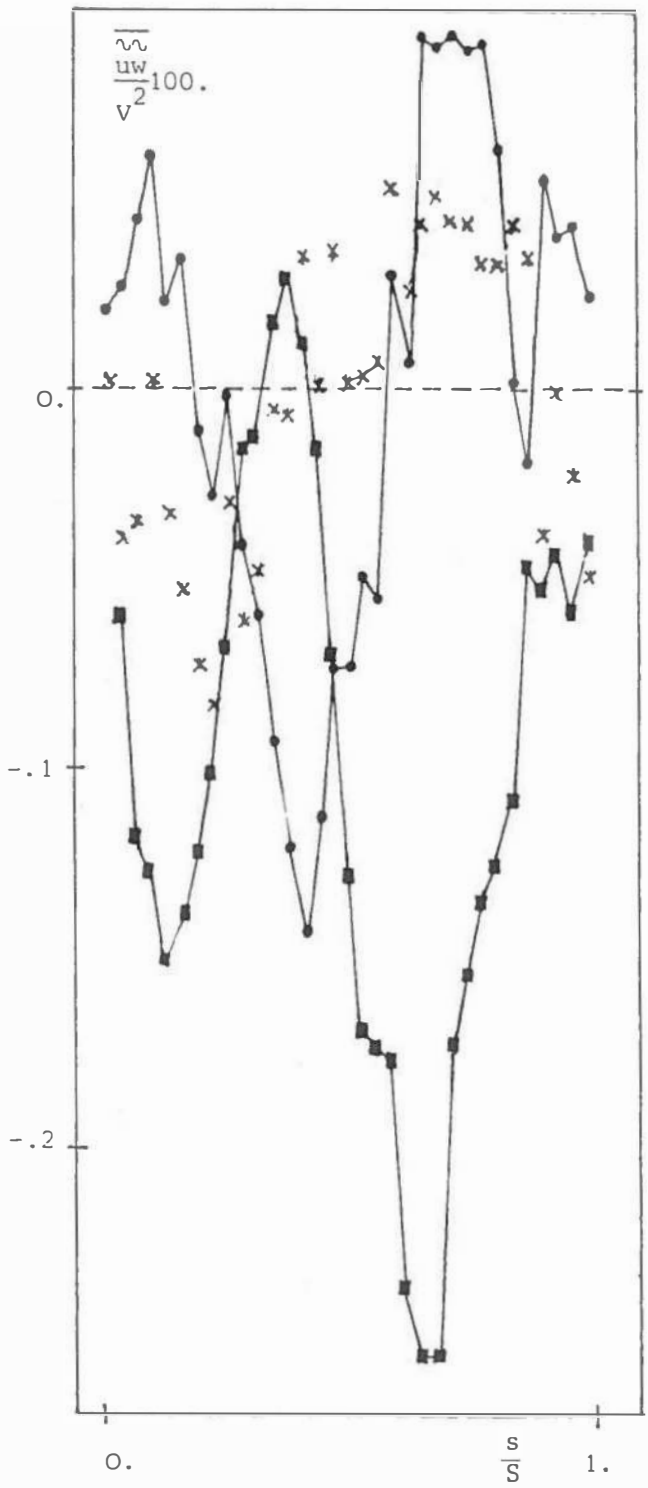

Fig. 13 Blade-to-blade distribution of the non-dimensional mixed stress, uw

Moreover, a high-performance mean-square meter is required as most of the signal power is concentrated near zero frequency, and a multichannel analyzer is required with more channels than are necessary for the averaging of the velocity

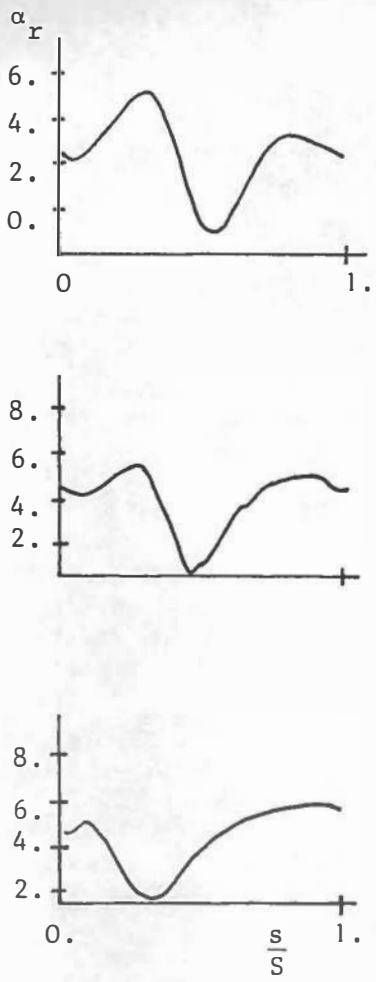

Fig. 14 Blade-to-blade distribution of the radial flow angle, α_r

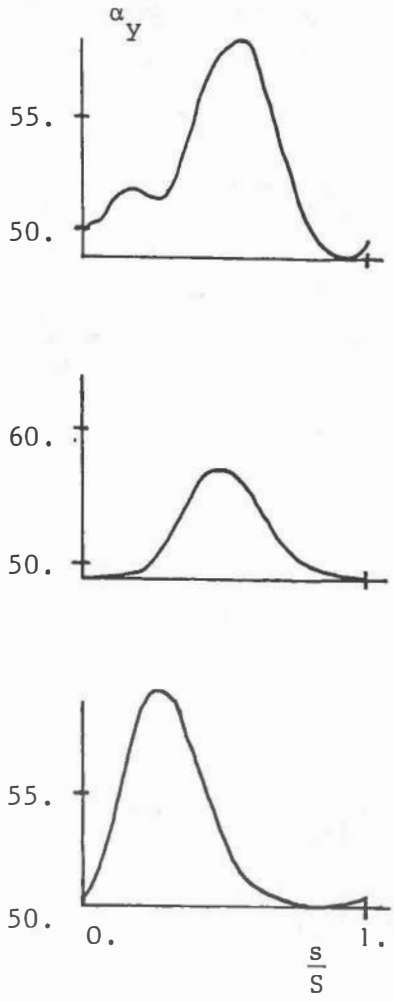

Fig. 15 Blade-to-blade distribution of the tangential flow angle, α_y

signal.

The stresses clearly reveal the presence of the blade-wake and other regions with non-uniform blade-to-blade velocity or angle profiles. Their relation with the average profiles is not straightforward, and detailed measurements close together in the axial and the radial direction are necessary to be able to calculate accurately the derivatives of these mean flow variables to compare these with the stresses.

ACKNOWLEDGMENT

The Von Karman Institute, Brussels, Belgium, is acknowledged for the facilities which have been offered to carry out these measurements.

REFERENCES

1 Gorton, C. A., and Lakshminarayana, B. A., "Method of Measuring the Three-Dimensional Mean Flow and Turbulence Quantities Inside a Rotating Turbomachinery Passage," ASME Paper No. 75-GT-4.

2 Kiock, R., "Turbulence Downstream of Stationary and Rotating Cascades," ASME Paper No. 73-GT-80.

3 Evans, R. L., "Turbulence and Unsteadiness Measurements Downstream of a Moving Blade Row," ASME Paper No. 74-GT-73.

4 Raj, R., and Lakshminarayana, B., "Three-Dimensional Characteristics of Turbulent Wakes Behind Rotors of Axial Flow Turbomachinery," ASME Paper No. 75-GT-4.

5 Eckardt, D., "Detailed Flow Investigations within a High Speed Centrifugal Impeller," ASME Paper No. 76-FE-13.

6 Colpin, J., and Kool, P., "Experimental Study of an Axial Compressor Rotor Transfer Function with Non-Uniform Inlet Flow," ASME Paper No. 78-GT-69.

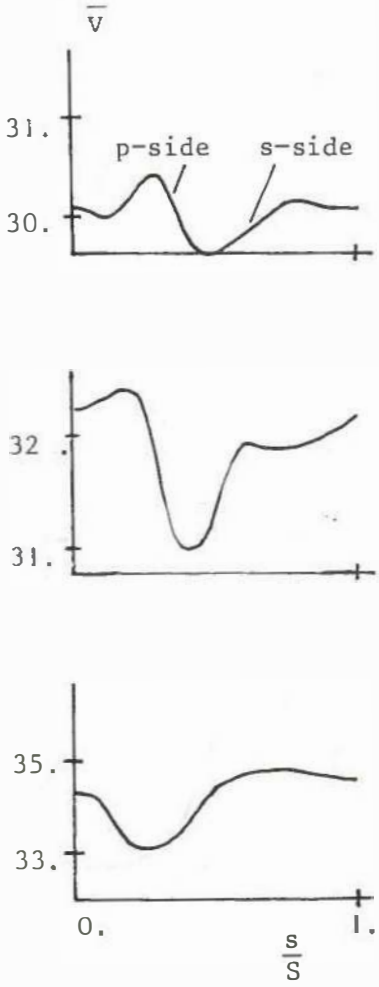

Fig. 16 Blade-to-blade distribution of the absolute velocity

7 Wagner, J. H., Okiishi, I. H., and Holbrook, G. J., "Periodically Unsteady Flow in an Imbedded Stage of a Multistage Axial-Flow Turbomachine," ASME Paper No. 78-GT-6.

8 Fujita, H., and Kovasznay, L. S. G., "Measurement of Reynolds Stress by a Single Rotated Hot-Wire Anemometer," Rev. Sci. Instr., Vol. 39, 1968, p. 1351.

9 Bissonnette, L. R., and Mellor, S. L., "Experiments on the Behaviour of an Axisymetric Turbulent Boundary Layer with a Sudden Circumferential Strain," J.F.M., Vol. 63, Part 2, April 1974.

10 De Grande, "Three-Dimensional Incompressible Turbulent Boundary Layers," Ph.D. Thesis Vrye Universiteit Brussel, 1977.

11 Kool, P., "Experimental Investigation of the Three-Dimensional Flow Field Downstream of Axial Compressors," Ph.D. Thesis Vrye Universiteit Brussel, Department of Fluid Mechanics, Jan. 1977.

12 Hirsch, Ch., and Kool, P., "Measurement of the Three-Dimensional Flow Field Behind an Axial Compressor Stage," Transactions of the ASME, Vol. 99, Series A, No. 2, 1977, p. 168.

13 Hirsch, Ch., and Kool, P., "Application of a Periodic Sampling and Averaging Technique to Flow Measurements in Turbomachines," Vrye Universiteit Brussel, Report No. VUB-STR-4, Sept. 1973.

14 Elgerd, O. I., Control Systems Theory, McGraw Hill, 1967.